Characterization of SiO_2 and Al_2O_3 Incorporated PVdF-HFP Based Composite Polymer Electrolytes with $LiPF_3(CF_3CF_2)_3$

V. Aravindan, P. Vickraman

Department of Physics, Gandhigram Rural University, Gandhigram 624 302, Tamilnadu, India

Received 9 August 2007; accepted 27 November 2007
DOI 10.1002/app.27824
Published online 23 January 2008 in Wiley InterScience (www.interscience.wiley.com).

ABSTRACT: Lithium fluoroalkylphosphate ($LiPF_3(CF_3CF_2)_3$) based composite polymer electrolytes (CPE) have been prepared in the matrix of polyvinylidenefluoride-hexafluoropropylene (PVdF-HFP), using solvent casting technique. The membranes were gelled with ethylene carbonate and diethyl carbonate as a plasticizer and nanosized SiO_2 and nanoporous Al_2O_3 as fillers. These membranes were subjected to a.c. impedance, DSC, SEM, FTIR, and Fluorescence studies. The a.c. impedance studies and activation energy calculation reveal that 2.5 wt % fillers containing membranes only exhibit maximum conductivity for SiO_2 (1.16 mS cm^{-1}) and Al_2O_3 (0.98 mS cm^{-1}), compared to fillers free membranes and beyond 2.5 wt % of such fillers the conductivity tends to decrease. The enhancement of conductivity has been explained in terms of Vogel-Tamman-Fulcher (VTF) theory. Molecular interactions by FTIR and local viscosity environment by fluorescence studies have been investigated. © 2008 Wiley Periodicals, Inc. J Appl Polym Sci 108: 1314–1322, 2008

Key words: LiFAP; nanocomposite; crystallinity; activation energy; electrolytes; lithium ion batteries; ionic conductivity

INTRODUCTION

In the last two decades, lithium solid polymer electrolytes (SPEs) have drawn significant worldwide attention for their commercial applications such as in high energy density batteries, electrochromic devices, and electrochemical sensors.[1] In spite of the worldwide interest, a series of technical issues have held the SPEs back from being commercially implemented. These include low ambient temperature conductivity, cationic transport number, inadequate thermal stability, and poor electrochemical performance of Li cells below room temperature. Some of the approaches pursued to achieve higher conductivity and better electrochemical performances of the SPEs are polymer structure modification by radiation to achieve crosslinking,[2] plasticization,[3] the addition of nanosized/nanoporous inorganic fillers,[4] and use of a large anion lithium salt.[5]

Till date, development of new generation ambient Li-ion batteries has been based almost exclusively on gel electrolytes.[6] Several organizations including Bellcore (now called Telcordia), Mead, Valence from USA, and Yuasa (Japan) have announced lithium batteries based on gel electrolytes. One of the remaining challenges in these systems is to increase the stability with the metal electrode and decrease the interfacial impedance as well as to replace $LiPF_6$. Gas evolution while cycling and poor mechanical strength questions the use of gel electrolytes in Li-polymer batteries. On the other hand, composite electrolytes, prepared by incorporating nanoparticles in a gel matrix not only gives raise to the expected high ambient conductivity of conventional gel electrolytes but also showing excellent stability toward the metal electrode and good mechanical strength. Thus the present work incorporates the behavior of gel polymer electrolytes as well as composite polymer electrolytes that constitutes what is called nanogel electrolytes (hereafter is called as CPE). These CPEs exhibit rubbery behavior. The rubbery behavior and compliance are important requirements for solid electrolytes during battery charging and discharging because of large volumetric changes. Moreover, the CPEs can also be processed at much higher temperature than the conventional gel electrolytes.[7,8]

In the recent years, the extensive research work is focused for the development of new lithium salts for lithium rechargeable batteries due to the drawbacks of commercially available salts namely $LiClO_4$ (is potentially explosive in contact with organics), $LiBF_4$ (interferes with the SEI at the graphite anode, but it has better thermal stability and lower sensitivity toward moisture than $LiPF_6$), $LiAsF_6$ (toxic), $LiSO_3CF_3$ (have too low conductivities), $LiN(SO_2CF_3)_2$, and $LiC(SO_2CF_3)_3$ do not effectively passivate the aluminum current collector at the positive electrode i.e.,

Correspondence to: P. Vickraman (vrsvickraman@yahoo.com).

severe corrosion toward the aluminum current collector,[9] and even some of the drawbacks of $LiPF_6$ in conventional lithium ion batteries at present.

In this regard an interesting new type of novel salt synthesized namely lithium fluoroalkylphosphate ($LiPF_3(CF_3CF_2)_3$) (LiFAP) of a large anion is used for first time for the preparation of CPE. The premise for LiFAP development is that the substitution of one or more fluorine atoms in $LiPF_6$ with electron-withdrawing perfluorinated alkyl groups should stabilize the P—F bond, rendering it to stable against hydrolysis. In fact, LiFAP exhibits good resistance against hydrolysis (Scheme 1). Thus the hydrophobic perfluorinated alkyl groups sterically shield the phosphorus against hydrolysis. Further the new compounds also have conductivity comparable to that of $LiPF_6$. The stabilization of the P—F bond results in an improved thermal stability of the salt. Oesten et al.[10] reported that $LiPF_3(CF_3CF_2)_3$ (LiFAP) exhibits a far superior stability toward hydrolysis and reduced flammability. These authors content that LiFAP has a combination of flame-retardant moieties, fluorinated derivatives, and phosphoric acid esters. Gnanaraj and coworkers[11–15] investigated the thermal stability of solutions of $LiPF_6$ and LiFAP in EC-DEC-DMC mixtures using accelerating rate calorimetry (ARC) and showed that the onset temperature for thermal reactions of LiFAP solutions are higher than 200°C ($LiPF_6$ solutions: <200°C) although their self-heating rate is very high.

MATERIALS AND METHODS

Materials

LiFAP was received from Merck KGaA, Germany as complexed with dimethoxy ether (DME) ($LiPF_3(CF_3CF_2)_3 \cdot 3DME$). Appropriate amount of salt is dissolved in binary mixture solvents (ethylene carbonate (EC) and diethyl carbonate (DEC) mixture with 1 : 1 weight ratio), which has the boiling point higher than DME. It is heated up to 90°C for the complete evaporation of DME, which was confirmed by FTIR studies. The materials EC, DEC, nanoporous (5.8 nm) acidic aluminum oxide (Al_2O_3) (with the surface area of 155 $m^2\ g^{-1}$), and tetrahydrofuran (THF) were procured with high purity grade from Aldrich (USA). PVdF-HFP with 12 mol % of HFP was obtained from Solvay Solexis, Italy. Silicon dioxide (SiO_2) nanoparticle (12 nm with the surface area of 200 $m^2\ g^{-1}$) was provided by Degussa, India. Polymer electrolyte membranes were prepared according to the composition of Table I by solvent casting technique.

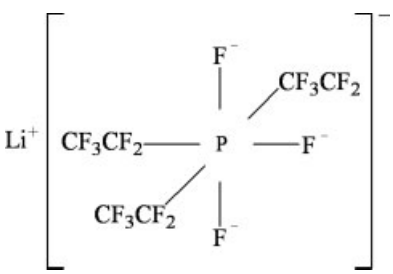

Scheme 1 Structure of LiFAP.

TABLE I
Composition of Polymer Electrolytes[a]

Sample	PVdF-HFP	Plasticizer EC	Plasticizer DEC	LiFAP	Al_2O_3/SiO_2
S1	30	32.50	32.50	5.00	00.0
S2	30	31.25	31.25	5.00	02.5
S3	30	30.00	30.00	5.00	05.0
S4	30	28.75	28.75	5.00	07.5
S5	30	27.50	27.50	5.00	10.0

[a] The combinations are in weight ratios.

Instrumentation

Ionic conductivities of LiFAP based membranes were carried out in the frequency range of 5 MHz–1 Hz by a.c. impedance spectroscopy using Solartron 1260 Impedance/Gain Phase analyzer coupled with a Solartron Electrochemical interface with two stainless steel blocking electrodes (SS/CPE/SS, where SS stainless steel) having 1 cm^2 area. The FTIR spectrum was recorded between 4000 and 400 cm^{-1} in the transmittance mode using a Jasco 460 Plus IR spectrophotometer with a resolution of 4 cm^{-1}. Morphological features of the membranes were examined by using a Hitachi Model S-3000H scanning electron microscope. Differential scanning calorimetry (DSC) traces were recorded using the Perkin-Elmer Pyris 6 in the Nitrogen atmosphere from 40 to 240°C with the heating scanning rate of 10°C/min. Perkin–Elmer LS 55 luminescence spectrometer was used for fluorescence measurements. The sample holder was placed 60° against the excitation wavelength and the emission and excitation wavelength were fixed for 360 and 280 nm, respectively.

RESULTS AND DISCUSSION

Conductivity studies

Electrochemical impedance spectroscopy is a relatively new and powerful method to characterize many of the electrical properties of materials and their interfaces with the electronically conducting electrodes. It may be used to investigate the dynamics of bound or mobile charge in the bulk or interfacial regions of any kind of solid or liquid material: ionic, semiconducting, mixed electronic–ionic, and even

insulators (dielectrics). The a.c impedance spectrum of a SS/CPE/SS symmetrical cell with equivalent electrical circuit is represented in Figure 1 and the response of the cell can be understood on the basis of the equivalent circuit. The impedance (Z) of the cell is given by

$$Z = \left(R_b - \frac{j}{2\pi f\, C_g}\right) + \left(R_i - \frac{j}{2\pi f\, C_i}\right) \quad (1)$$

where R_i and R_b are resistance of the SS/CPE/SS interphase and the resistance of the SS/CPE interphase and the geometric capacitance of the CPE, respectively; f, the ac frequency. On the right hand side of eq. (1), the impedance of the CPE is given in the first parenthesis and the impedance of the SS/CPE interphase is given in second parenthesis. Impedance spectrum which is expected theoretically from eq. (1) is shown in Figure 1 with two semicircles. The frequency range of each semicircle depends on the RC time constant of the resistance and the capacitance pair. From the literatures based on lithium based polymer electrolytes, the high frequency semicircle is attributed to the polymer electrolyte and the low frequency semicircle to the electrode/electrolyte interphase. The conductivity (σ) of the CPE can be calculated from the following equation,

$$\sigma = \frac{l}{AR_b} \quad (2)$$

where l, thickness of the CPE; A, area of the stainless steel (SS) electrode; and R_b, bulk resistance of the CPE.

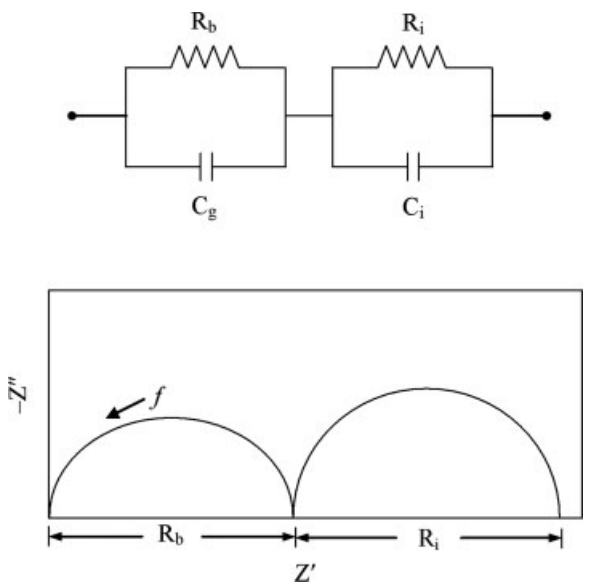

Figure 1 Electrical equivalent circuit of SS/CPE/SS cell and the corresponding impedance spectrum. The symbols R_b and R_i refer to the resistance of the CPE and resistance of the SS/CPE interphase; C_g and C_i refer to capacitance of the CPE and capacitance of the SS/CPE interphase, respectively.

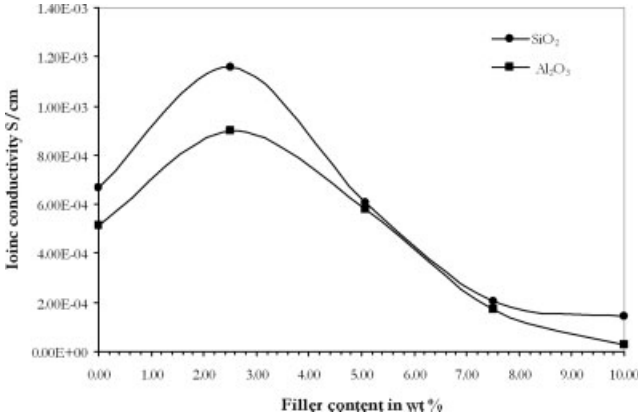

Figure 2 Variation of ionic conductivity of PVdF-HFP/(EC + DEC)/LiFAP based polymer gel electrolytes complexed with (a) SiO_2 nanoparticle and (b) acidic Al_2O_3 nanoporous fillers at room temperature.

The variation of ionic conductivity has been analyzed for LiFAP salt by varying the filler content (SiO_2 and Al_2O_3) with respect to the plasticizer content, (EC/DEC) for fixed polymer (PVdF-HFP) content. Figure 2 shows that ionic conductivity varies with different filler concentrations. It could be seen that conductivity of the filler-free membrane is 0.669 mS cm^{-1}. The conductivity increases for a filler content of 2.5 wt %, such that 1.16 mS cm^{-1} for SiO_2 and 0.980 mS cm^{-1} for Al_2O_3. A fall in conductivity is noted beyond 2.5 wt %. The drop in conductivity with increasing filler content may be attributed to an aggregation of fillers, strongly impeding polymer chain movement. These results are in agreement with our previous findings of LiBOB based polymer membranes.[16,17] Nan et al.[8] in their studies with CPEs comprising of PEO + EC/PC + $LiClO_4$ + SiO_2 showed that a conductivity maximum occurred at an SiO_2 level of 15 wt %. Although the nature of the filler material has an important influence on the conductivity behavior, other factors should also come into play preferably the nature of the anion used because for ClO_4^- system the SiO_2 used was 15 wt %, while in our case the SiO_2/Al_2O_3 were 2.5 wt % due to the bulkier size of the FAP anion. The bulky and weakly coordinating FAP^- anion may be expected to act as a strong plasticizer, lowering the amount of filler material required to obtain reasonable conductivity values. Moreover, the strong polarizing effect of the bulkier FAP^- anion can also influence charge transport. Figure 3 presents plots of conductivity versus $1/T$ for the CPEs. The plot shows that ionic conduction in the polymer electrolyte obeys the VTF (Vogel-Tamman-Fulcher) relation, which describes the transport properties in a viscous polymer matrix.[18]

The temperature dependence of ionic conductivity of CPEs are studied. It could be seen that a CPE containing 2.5 wt % filler exhibits a conductivity of

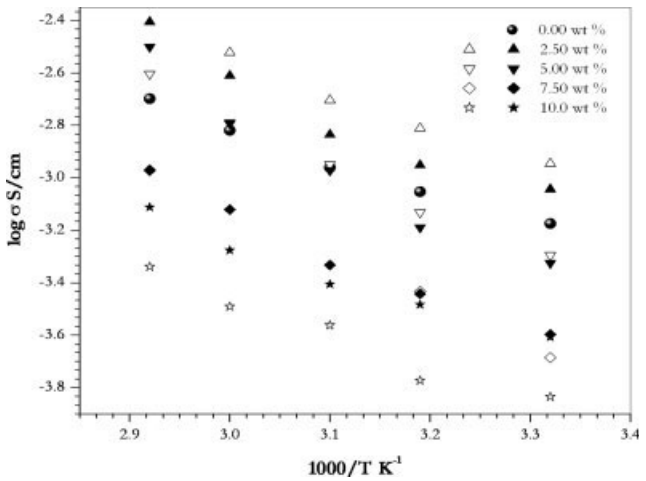

Figure 3 Temperature dependence ionic conductivity of PVdF-HFP/(EC + DEC)/LiFAP based polymer electrolytes incorporated with SiO_2 nanoparticle (open) acidic and Al_2O_3 nanoporous fillers (filled).

3.16 mS cm^{-1} for SiO_2 and 2.12 mS cm^{-1} for Al_2O_3 at 70°C. An increase in temperature leads to an increase in conductivity is observed, because as the temperature increases the polymer expands to produce free volume, which leads to enhanced ionic and polymer segmental mobilities. The enhancement of ionic conductivity with filler particles can be explained by the fact that the particles inhibit recrystallization kinetics, helping to retain the amorphous phase down to relatively low temperatures. At the same tine, plasticizers contribute to conductivity enhancement by opening up narrow rivulets of plasticizer-rich phases for greater ionic transport, generating large free volumes of relatively enhanced conducting phases.[19] It is observed that the magnitude of conductivity for SiO_2 system is slightly higher than Al_2O_3 based CPEs, it may be due to the lower particle size which gives raise to higher surface area.

Activation energy for Li^+ ion transport

Figure 3 exhibits the ionic conductivities dependence on the temperature ranging from 27 to 70°C for polymer electrolyte. This temperature dependence variation appears linear so that the activation energy for ions transport E_a can be further obtained by the VTF model

$$\sigma = \sigma_0 T^{-1/2} \exp\left(\frac{-E_a}{T - T_0}\right) \quad (3)$$

where σ, the conductivity of polymer electrolyte; σ_0, the pre-exponential index; T, the testing temperature; and T_0, glass transition temperature, respectively. Figure 4 shows the relationship between the amount of filler in the membrane and the activation energy

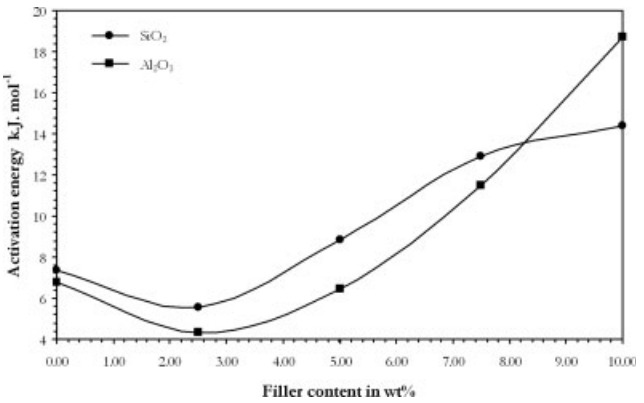

Figure 4 Activation energy for PVdF-HFP/(EC + DEC)/LiFAP based polymer electrolytes complexed with (a) SiO_2 nanoparticle and (b) acidic Al_2O_3 nanoporous fillers.

for ionic transport. This study suggests that the activation energy for ionic transport decreases as the filler concentration increases for filler levels up to 2.5 wt %. However, at higher filler levels (beyond 2.5 wt %), the activation energy increases. The reason for the increase in activation energy beyond 2.5 wt % may be due to the strong interaction between the ceramic particles and the polymer chains.

Thermal studies

DSC traces of PVdF-HFP films filled with different contents of filler particles (Al_2O_3/SiO_2) were measured to investigate the change in polymer crystal properties due to filler addition (Fig. 5). As the Al_2O_3 content increases, the T_m of cast film suffers

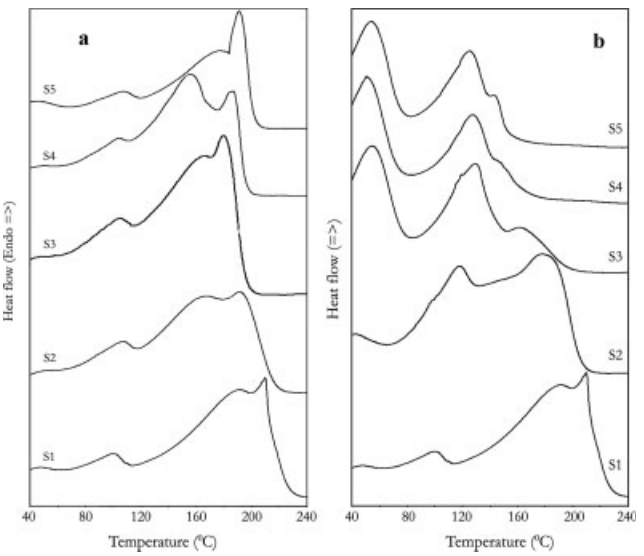

Figure 5 Differential scanning calorimetric traces of PVdF-HFP/(EC + DEC)/LiFAP based polymer electrolytes complexed with (a) SiO_2 nanoparticle and (b) acidic Al_2O_3 nanoporous fillers.

an irregular pattern of decrease and increase. This behavior is related to the crystal phases of VdF during heating and melting.[20] The films exhibit some melting peaks corresponding to VdF crystals (e.g., α- and γ-phases) in the range of 120–190°C, corresponding to the melting of the α-phase (big spherulite) crystals. The peak around 100°C in the filler-free electrolyte may be due to boiling of DEC. By adding 2.5 wt % of nanoporous Al_2O_3, the T_m shifted to a lower temperature, which leads to a decrease in crystallinity. Furthermore, increasing the filler content up to 10 wt %, a broad T_m starts at around to 128°C (the onset temperature of T_m starts at around 85°C), which includes the boiling point of DEC and the T_m of VdF crystals α-phase crystals. At the same time a small kink around 165°C may be due to the existence of the same α-phase crystals. The slight shift of T_m or the small change of crystal phase brought about by the addition of Al_2O_3 can be understood in terms of a localized influence on the polymer chain conformation resulting from some dipole orientation properties of Al_2O_3. Similar type of DSC profiles [Fig. 5(a)] have been observed for SiO_2 based CPEs, the endothermic event at around 60°C may be due to the absorption of moisture during the loading of the film.[21] The Al_2O_3 based CPEs exhibit exothermic events observed around 80°C which might be due to the nanocrystalline phase changes of Al_2O_3.[22]

SEM analysis

The opacity of the film is increased by increasing the filler content. Figure 6 shows the SEM images of CPEs with 0, 2.5, and 5.0 wt % of SiO_2 and Al_2O_3 fillers. The filler-free membrane shows a highly porous

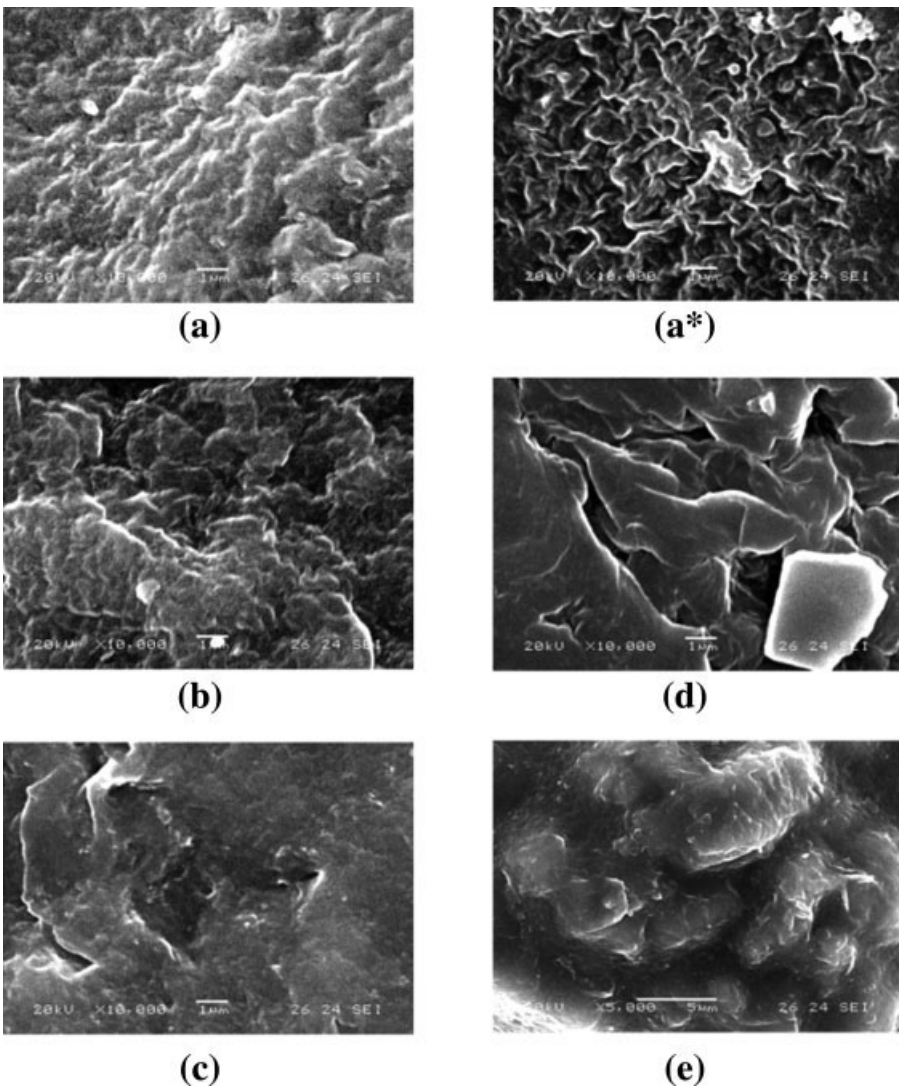

Figure 6 SEM images of PVdF-HFP/(EC + DEC)/LiFAP based polymer electrolytes. (a and a*) filler free membrane, (b) 2.5 wt % and (c) 5.0 wt % of SiO_2 nanoparticle; and (d) 2.5 wt % and (e) 5.0 wt % of acidic Al_2O_3 nanoporous filler.

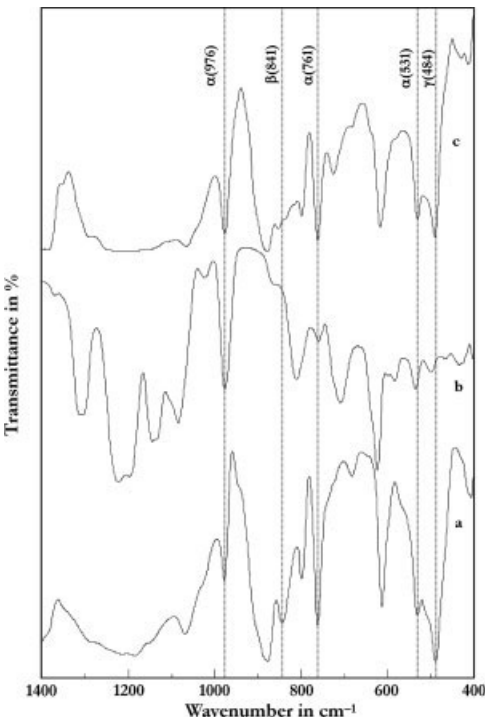

Figure 7 FTIR spectrums of (a) PVdF-HFP, (b) LiFAP, and (c) PVdF-HFP + LiFAP.

structure [Fig. 6(a,a*)]. The presence of pores may be due to the accumulation of the plasticizer between the interconnected networks of the polymer matrix. Addition of a small amount, say, 2.5 wt % of the filler, leads to an improvement in the morphology of the membrane. Upon increasing the filler content to 5 wt %, the filler particles get unevenly dispersed in the matrix, resulting in an aggregation of the particles which impede ionic conduction in Figure 3.

Generally, conductivity in conventional polymer electrolytes is achieved through continuous pathways of absorbed liquid electrolyte within interconnected pores of membranes. Thus, a highly developed porous structure is a prerequisite for a good ionically conducting separator.[23] It is, therefore, clear that in such a structure, ionic conductivity of the electrolyte is a major determinant. Thus, the conductivity of an electrolyte-laden membrane is influenced by membranes porosity, tortuosity of the pores, the conductivity of the liquid electrolyte, the thickness of the membrane, and the extent of wetting of the membrane by the electrolyte. In the case of composite electrolytes, the porous structure of the membranes tend toward a nonporous one when filler concentrations exceed 2.5 wt %, as is evident from a

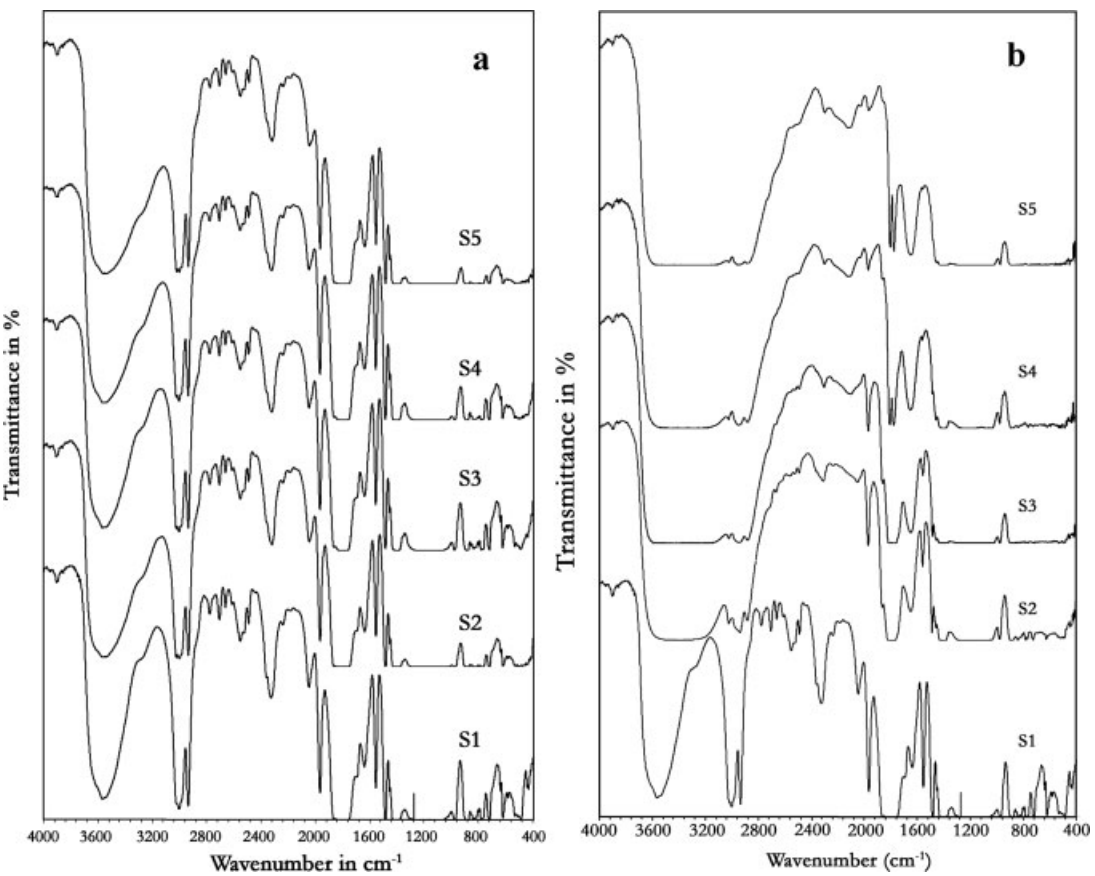

Figure 8 FTIR spectrum of CPE having different filler contents (a) (S1) 0 wt %, (S2) 2.5 wt %, (S3) 5.0 wt %, (S4) 7.5 wt %, and (S5) 10 wt % of SiO_2 nanoparticles; (b) (S1) 0 wt %, (S2) 2.5 wt %, (S3) 5.0 wt %, (S4) 7.5 wt %, and (S5) 10 wt % of nanoporous Al_2O_3.

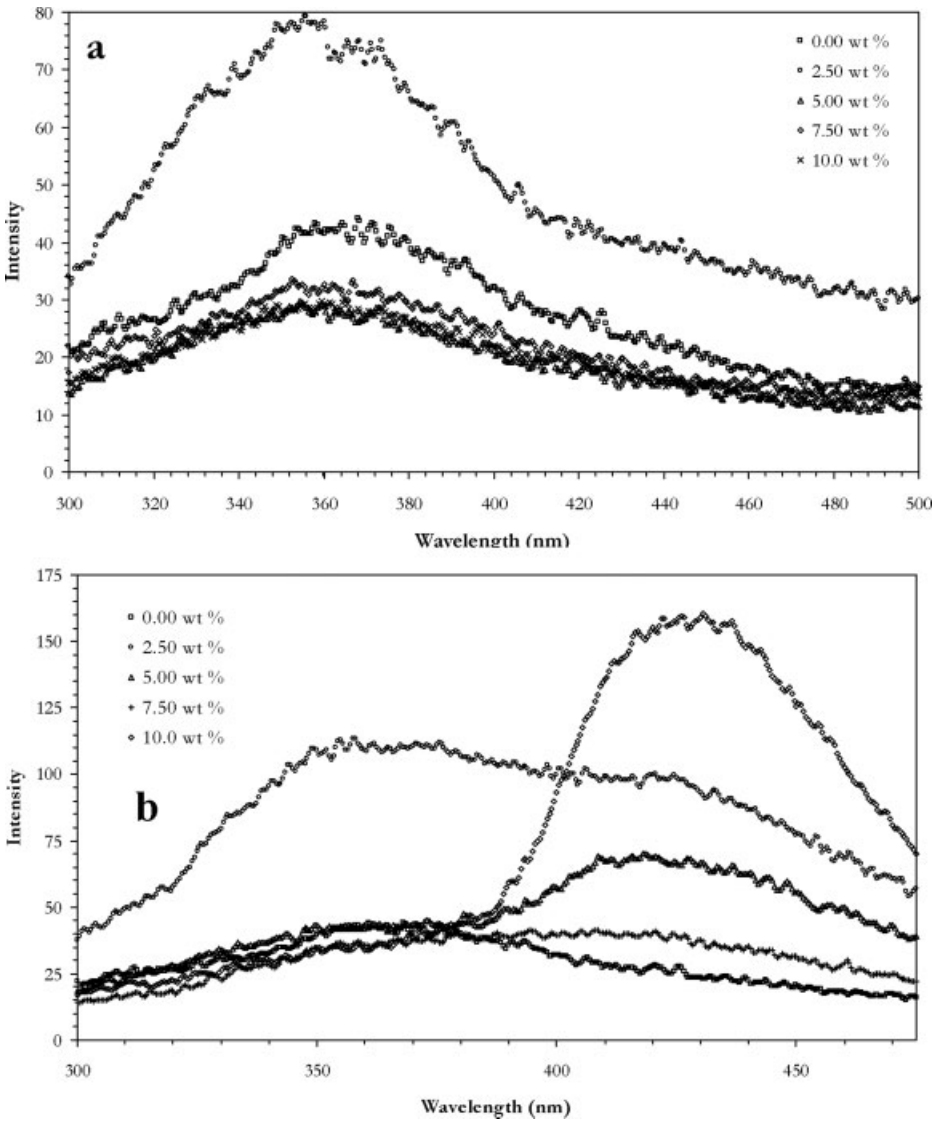

Figure 9 Fluorescence excitation spectrum for SiO_2 (a) and Al_2O_3 (b) based CPE comprising different filler contents.

drop in conductivity above this filler loading. In the case of SiO_2 based CPEs, CPEs look gel type appearance at 2.5 wt % filler content which exhibits slightly higher conductivity than Al_2O_3

FTIR studies

FTIR is a powerful tool to study the local structural changes. Complexation may shift/diminishing intensities in the polymer cage peak frequencies. The infrared spectra would be sensitive both in situations where complexation has occurred in crystalline or amorphous phase. FTIR spectra of the samples were recorded in the transmittance mode. The FTIR spectrum in Figure 7 is evidence for interactions between the polymer host and LiFAP salt. Characteristic vibrational bands of PVdF-HFP at 531, 766, and 976 cm^{-1}, corresponding to the α phase crystals are clearly seen. There are, in addition, bands at 484 and 841 cm^{-1} corresponding, respectively, to the β and γ phases.[24] The bands at 839 and 879 cm^{-1} correspond to the amorphous phase of the polymer. The band around 613 cm^{-1} is assigned to —C—F— wagging mode and those around 1197 and 1276 cm^{-1} correspond to asymmetric and symmetrical stretching vibrations of the $—CF_2$ group. Peaks at wave numbers 1185 and 1069 cm^{-1} are assigned to the symmetrical stretching mode of $—CF_3$ and $—CF_2$ groups, respectively, in the pure polymer.[25] That at 1303–1025 cm^{-1} is assigned to —C—F— and $—CF_2$ stretching vibrations of LiFAP. The bands 758 and 709 cm^{-1} are assigned to $—CF_3$ bending and —C—F— wagging modes of fluoroalkyl group. The peaks at 810 and 976 cm^{-1} are assigned to P—F bonds and —C—C— bonds respectively, while those at 496 and 535 cm^{-1} correspond, to the wagging and bending vibrations of

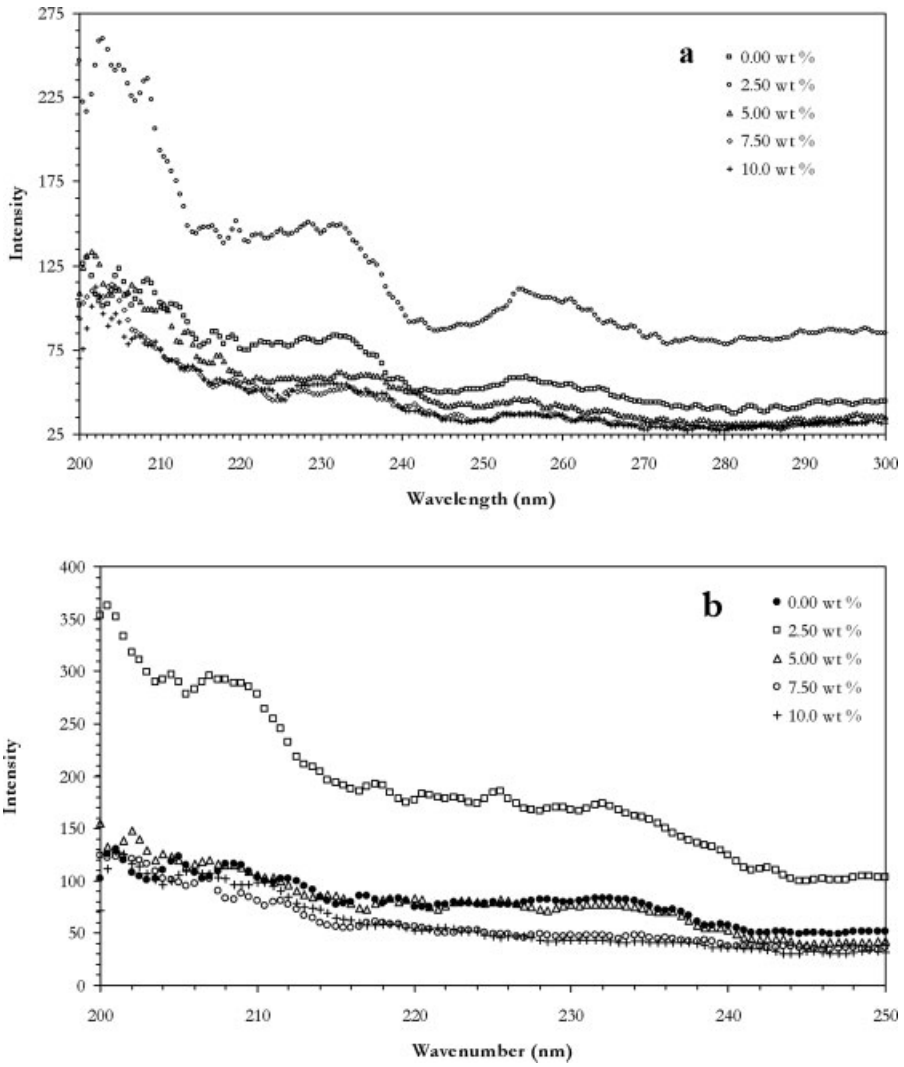

Figure 10 Fluorescence emission spectrum for SiO_2 (a) and Al_2O_3 (b) based CPE comprising different filler contents.

$—CF_2$ groups. Figure 8 shows the FTIR spectra of CPEs with different filler contents. A comparison of Figures 7 and 8 suggests complex formation and interactions involving the constituents of the polymer electrolyte. In Figure 8(a), the bands at 3010 and 2967 cm^{-1} are assigned to CH_3 and CH_2 stretching regions of DEC is shifted and decreased in magnitude which was observed in the all CPEs. This suggested that the interaction of solvent molecules with surface group of the SiO_2 nanoparticle. CH_2 bending mode of (1479 cm^{-1}) is observed only in filler free and 2.5 wt %. Ring breathing mode of EC is obviously observed at 976 cm^{-1} in all the electrolytes with decrease in intensity after the loading of SiO_2. The bands of DEC at 895 (—OCOO— out of plance deformation), 855 (CH_2 rocking) and 793 cm^{-1} (out of plane skeleton deformation) is diminished after the addition of SiO_2 nanoparticles.[26] Similarly, the drastic decrease in CH_2 bending mode (1480 cm^{-1}) of EC is decreased after the addition of 2.5 wt % of SiO_2, it was diminished by further addition of fillers. EC bands at 1865 (C=O stretching), 1394 (CH_2 wagging) and 720 (C=O bending) were observed for filler free and 2.5 wt % membranes only.[27] Similar type of interactions has also been observed for Al_2O_3 based CPEs [Fig. 8(b)]. The diminishing of such intensities is not only due to surface interactions of the nanoporous Al_2O_3/SiO_2 nanoparticle, also interaction with $—CF_2$ group of polymer as well the flouroalkyl group of LiFAP.

Fluorescence studies

Ionic mobility in porous structures cannot be correlated directly with the macroscopic viscosity measured usually by rheometric methods.[28] In fact, ionic mobility in these structures is related to the local viscosity surrounding the charge carriers. Fluorescence studies provide information on local viscosity effects in polymeric media. This technique can also detect structural alterations in the local environments and

has been used to study the structural, conformational, and dynamic properties of polymer systems.[29,30] The intensity values are directly proportional to the local viscosity of the surrounding polymeric media.

Typical fluorescence emission and excitation spectra of CPEs with different filler loadings are given in Figures 9 and 10. It can be seen that the CPE with 2.5 wt % filler concentration shows a higher intensity than the other membranes. This suggests that molecular motion in composite polymer systems is hindered above certain filler concentrations. The higher viscosities of the polymeric medium leads to decrease in mobility of the ions, which translates into reduced conductivity. The enhancement in local viscosity may be attributed to a strong interaction between the filler particles and the polymer host, resulting in sluggish segmental motion of polymer chains.

CONCLUSIONS

LiFAP based CPEs have been synthesized. The characterization studies on such electrolytes reveal that an appealing moderate conductivity of 10^{-3} S cm^{-1} has been observed for 2.5 wt % of fillers. Thus, the present study gives an insight about the importance of nature of fillers and the nature of anion and the interaction between them. The thermal studies brings forth basic understandings about the fillers that it reduces the T_m of the polymeric membrane to lower temperatures (as much as 85°C at a filler concentration of 2.5 wt %). The lowering of the crystalline nature of the CPEs leads to improved conductivity. The FTIR and SEM studies confirm the degree of complexation of constituents of the polymer electrolytes. The fluorescence studies supplements the filler particles participation for the local viscosity changes in the polymeric matrix. Thus, all these studies convincingly prove that LiFAP based SiO_2 and Al_2O_3 CPEs may certainly be potential candidates for future lithium ion batteries replacing $LiPF_6$.

One of the authors (V.A.) is grateful to Prof. Nikolai Ignatyev and Dr. Winfried Geissler, Ionic Liquids Research Laboratory, Merck KGaA, Darmstadt, Germany, Mr. Vikas Rane, Degussa (India) Pvt. Ltd., Mumbai, and Anna Maria Bertasa, Solvay Solexis S.p.A., Italy for their timely help.

References

1. Gray, F. M. Polymer Electrolytes. The Royal Society of Chemistry: England, 1997.
2. Song, Y.; Peng, X.; Lin, Y.; Wang, B.; Chen, D. Solid State Ionics 1995, 76, 35.
3. Abraham, K. M.; Alamgir, M. J Electrochem Soc 1990, 137, 1657.
4. Croce, F.; Appetecchi, G. B.; Persi, L.; Scrosati, B. Nature 1998, 394, 456.
5. Appetecchi, G. B.; Henderson, W.; Villano, P.; Berrettoni, M.; Passerini, S. J Electrochem Soc 2001, 148, A1171.
6. Croce, F.; Curini, R.; Martinelli, A.; Persi, L.; Ronci, F.; Scrosati, B.; Caminiti, R. J Phys Chem B 1999, 103, 10632.
7. Jacob, M. M. E.; Hackett, E.; Giannelis, E. P. J Mater Chem 2003, 13, 1.
8. Nan, C. W.; Fan, L.; Lin, Y.; Cai, Q. Phys Rev Lett 2003, 91, 266104.
9. Balakrishnan, P. G.; Ramesh, R.; Prem Kumar, T. J Power Sources 2006, 155, 401.
10. Oesten, R.; Heider, U.; Schmidt, M. Solid State Ionics 2002, 148, 391.
11. Gnanaraj, J. S.; Zinigrad, E.; Asraf, L.; Sprecher, M.; Gottlieb, H. E.; Geissler, W.; Schmidt, M.; Aurbach, D. Electrochem Commun 2003, 5, 946.
12. Gnanaraj, J. S.; Levi, M. D.; Gofer, Y.; Aurbach, D.; Schmidt, M. J Electrochem Soc 2003, 150, A445.
13. Aurbach, D.; Gnanaraj, J. S.; Geissler, W.; Schmidt, M. J Electrochem Soc 2004, 151, A23.
14. Gnanaraj, J. S.; Zinigrad, E.; Levi, E.; Aurbach, D.; Schmidt, M. J Power Sources 2003, 119–121, 799.
15. Zinigrad, E.; Asraf, L.; Gnanaraj, J. S.; Gottlieb, H. E.; Sprecher, M.; Aurbach, D. J Power Sources 2005, 146, 176.
16. Aravindan, V.; Vickraman, P. J Phys D Appl Phys 2007, 40, 6754.
17. Aravindan, V.; Vickraman, P.; Prem Kumar, T. J Membr Sci 2007, 305, 146.
18. Wang, H.; Huang, H.; Wunder, S. L. J Electrochem Soc 2000, 147, 2853.
19. Rhoo, H. J.; Kim, H. T.; Park, J. M.; Hwang, T. S. Electrochim Acta 1997, 42, 1571.
20. Sajkiewicz, P. Eur Polym J 1999, 35, 1581.
21. Kim, K. M.; Park, N. G.; Ryu, K. S.; Chang, S. H. Electrochim Acta 2006, 51, 5636.
22. Aravindan, V.; Vickraman, P. Eur Polym J 2007, 43, 5121.
23. Song, J. Y.; Wang, Y. Y.; Wan, C. C. J Electrochem Soc 2000, 147, 3219.
24. Gregorio R., Jr.; Cestari, M. J Polym Sci B 1994, 26, 859.
25. Li, Z.; Su, G.; Gao, D.; Wang, X.; Li, X. Electrochim Acta 2004, 49, 4633.
26. Wang, J.; Wu, Y.; Xuan, X.; Wang, H. Spectrochim Acta A 2002, 58, 2097.
27. Osman, Z.; Arof, A. K. Electrochim Acta 2003, 48, 993.
28. Park, U. S.; Hong, Y. J.; Oh, S. M. Electrochem Acta 1993, 41, 849.
29. Waldow, D. A.; Ediger, M. D.; Tamaguchi, T.; Matsushita, T.; Noda, E. Macromolecules 1991, 24, 3147.
30. Kim, C. S.; Oh, S. M. J Power Sources 2002, 109, 98.